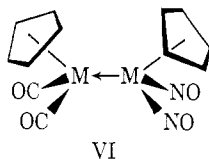


present case is probably less than 15 kcal/mol (19 kcal/mol - ΔH_2). However, it has been noted⁵⁴ that variation of R has a marked effect on rates of cis-trans isomerization in $(C_5H_5)Mo(CO)_2(L)R$ compounds, and it is conceivable that the adjacent transition metal could lower the barrier to polytopal isomerization in $[(C_5H_5)ML_2]_2$ systems. The second plausible mechanism for cis-trans equilibration is an *unsymmetrical* cleavage of the bridging ligands, to leave two carbonyls on one manganese and two nitrosyls on the other (VI). In valence bond terms, this



intermediate contains a metal-metal dative bond, for which there is some precedent.⁵⁵

The kinetic parameters follow a smooth trend across the periodic table, as can be seen in Table VI. The

(54) J. W. Faller and A. S. Anderson, *J. Amer. Chem. Soc.*, **92**, 5852 (1970).

(55) R. Hoxmeier, B. Deubzer, and H. D. Kaesz, *J. Amer. Chem. Soc.*, **93**, 536 (1971); M. R. Churchill and M. V. Veidis, *Chem. Commun.*, 529 (1970); W. E. Douglas, M. L. H. Green, C. K. Prout, and G. V. Rees, *ibid.*, 896 (1971).

activation energies for bridge-terminal ligand interchange and cis-trans equilibration decrease in the order Cr > Mn > Fe. For the latter two systems bridge-terminal ligand interchange is more rapid for the trans than for the cis isomer ($\Delta H_3^t < \Delta H_3^c$). It was not possible to obtain such information for $[(C_5H_5)Cr(NO)_2]_2$. The trend in ΔH_3 may well represent the decrease in energy necessary to break nitrosyl as compared with carbonyl bridges, although changes in ΔH_2 as well as strain in the bridge must also be important. These data are incorporated in the comparative reaction coordinates of Figure 9.

Acknowledgments. We are grateful to the National Science Foundation for support of this work. The R20-B nmr spectrometer was purchased with funds from NSF and E. I. Dupont and Co. We thank Professor Victor Day of the University of Nebraska for structural data in advance of publication.

Supplementary Material Available. Tables II and III and final values of $|F_o|$ and $|F_c|$ will appear following these pages in the microfilm edition of this volume of the journal. Photocopies of the supplementary material from this paper only or microfiche (105 × 148 mm, 20 × reduction, negatives) containing all of the supplementary material for the papers in this issue may be obtained from the Journals Department, American Chemical Society, 1155 16th St., N.W., Washington, D. C. 20036. Remit check or money order for \$3.00 for photocopy or \$2.00 for microfiche, referring to code number JACS-73-6602.

Mössbauer Spectra of Iron Complexes with Macrocylic Ligands. Partial Center Shifts and Partial Quadrupole Splittings

James C. Dabrowiak,^{1a} Philip H. Merrell,^{1a}
John A. Stone,^{1b} and Daryle H. Busch*^{1a}

*Contribution from the Evans Chemical Laboratory,
The Ohio State University, Columbus, Ohio 43210,
and the Savannah River Laboratory, E. I. du Pont de Nemours and Company,
Aiken, South Carolina 29801. Received April 11, 1973*

Abstract: Mössbauer spectra have been measured and interpreted in detail for 37 iron complexes with synthetic macrocylic tetradentate ligands. Most of the complexes are six-coordinate derivatives of the composition $Fe^{II-III}(MAC)X_2^{n+}$. The macrocylic ligands (MAC) vary in ring size and in the extent and arrangement of unsaturated linkages; the axial ligands X may be CH_3CN , imidazole, NCS^- , CN^- , NO_2^- , Cl^- , Br^- , I^- , or $CH_3CO_2^-$. Two oxo bridged dimers $(MAC)FeOFe(MAC)^{n+}$ were also studied. The center shift, δ , and quadrupole splitting, ΔE_q , for the ligating groups involved in the six-coordinate low-spin iron(II) complexes have been separated into additive quantities, the partial center shift (pcs) and the partial quadrupole splitting (pqs). These quantities correlate with spectrochemical parameters determined for other ions (Co^{III} and Ni^{II}) and with the limited data available for iron(II) itself; from these correlations, spectrochemical parameters or ligand field strengths that are not directly measurable can be estimated for a number of ligands that form important complexes with iron. The pcs and pqs values indicate the importance of π bonding in Fe^{II} complexes with the α -diimine linkage and support the view that ΔE_q is largely a function of $Dq_{xy} - Dq_z$. The relationship of Mössbauer data on iron hemes to that of the relatively simple model system of this report is discussed.

Iron complexes of synthetic macrocylic ligands have been produced and characterized recently.²⁻⁷ Al-

though similar macrocylic compounds of copper, nickel, and cobalt are well-known and have been

(1) (a) Evans Chemical Laboratory, The Ohio State University.
(b) Savannah River Laboratory, E. I. du Pont de Nemours and Co.

(2) V. L. Goedken, P. H. Merrell, and D. H. Busch, *J. Amer. Chem. Soc.*, **94**, 3397 (1972).

(3) V. L. Goedken and D. H. Busch, *J. Amer. Chem. Soc.*, **94**, 7355 (1972).

(4) J. C. Dabrowiak, P. H. Merrell, and D. H. Busch, *Inorg. Chem.*, **11**, 1979 (1972).

(5) J. C. Dabrowiak and D. H. Busch, unpublished results.

(6) V. Katovic and D. H. Busch, unpublished results.

(7) K. Travis, Thesis, The Ohio State University, 1970.

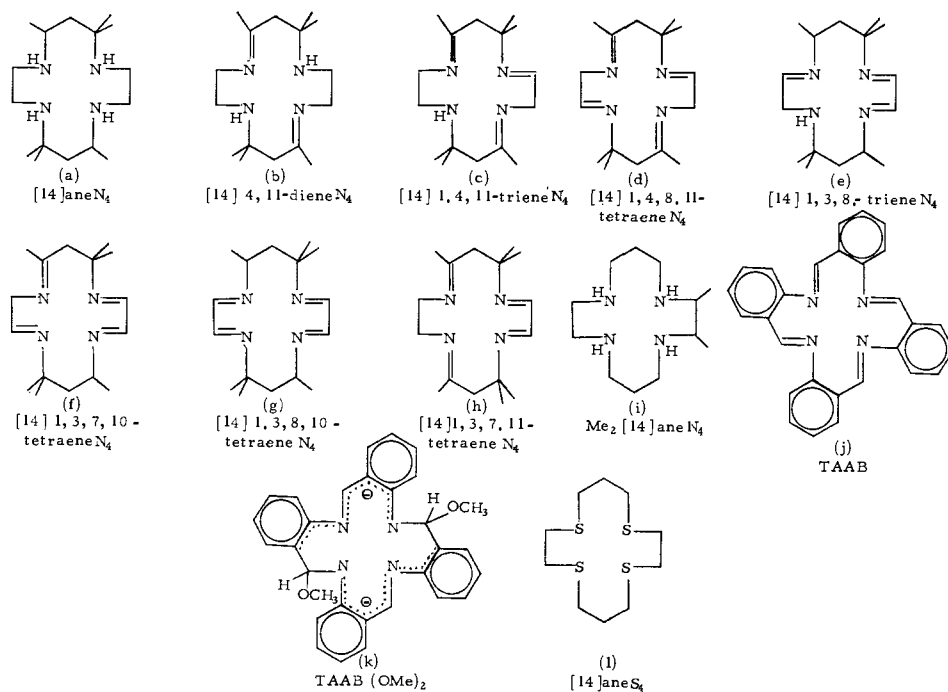


Figure 1. The abbreviations give the size of the ring in brackets followed by the number and location of unsaturated groups in the ligand.

studied in great detail,⁸ considerably less is known of the iron complexes. Because they are synthetic analogs of natural products such as the porphyrins, the iron macrocyclic compounds are especially attractive candidates for detailed studies of structure and bonding. In addition to the usual methods of characterization, the presence of iron in these compounds permits studying them by Mössbauer spectroscopy. In an earlier report⁹ Mössbauer data were given for several five-coordinate high-spin iron(II) synthetic macrocyclic complexes. We have now extended these Mössbauer studies to a wide variety of six-coordinate macrocyclic compounds of low-spin and high-spin iron(II) and low-spin iron(III).

Interpretation of the Mössbauer data is aided by the concept of partial center shifts (pcs) and partial quadrupole splittings (pqs). In principle these additive quantities may be assigned to each ligand, so that the total shift or splitting for any combination of ligands attached to a central Mössbauer-active atom may be calculated. Assignment of pcs values for ligands bonding to iron was first attempted by Herber, King, and Wertheim.¹⁰ In recent work by Bancroft, Mays, and Prater,¹¹ both pcs and pqs values are given for a large number of ligands bonded to six-coordinate low-spin iron(II). Many of the macrocyclic complexes in the present study contain iron in this configuration; these systems are well suited for testing and extending the theory of partial center shifts and partial quadrupole splittings, thereby gaining new insights into the structure and bonding of the complexes.

The Mössbauer center shifts and quadrupole splittings

(8) D. H. Busch, K. Farmery, V. Goedken, V. Katovic, A. C. Melnyk, C. R. Sperati, and N. Tokel, *Advan. Chem. Ser.*, No. 100, 44 (1971).

(9) P. H. Merrell, V. L. Goedken, D. H. Busch, and J. A. Stone, *J. Amer. Chem. Soc.*, **92**, 7590 (1970).

(10) R. H. Herber, R. B. King, and G. K. Wertheim, *Inorg. Chem.*, **3**, 101 (1964).

(11) G. M. Bancroft, M. J. Mays, and B. E. Prater, *J. Chem. Soc. A*, 956 (1970).

are given for the iron complexes of the broad series of synthetic tetradentate macrocyclic ligands shown in Figure 1. With the exception of two of the complexes with the ligand abbreviated as TAAB, the compounds contain a cyclic tetradentate ligand coordinated in a planar fashion, with two monodentate ligands occupying axial sites above and below the plane of the metal ion and the four nitrogen donor atoms. The majority of these materials have been characterized previously, using a variety of physical methods.²⁻⁷ However, for the full development of the concepts presented in this paper, several new complexes were synthesized. Some of these compounds were produced by simple metathetical procedures from well-identified starting materials, and only the essential physical data are presented here.

Seven of the macrocyclic ligands (Figure 1, a-g) used in this investigation have the same basic carbon skeleton, but each has a different number and/or arrangement of imine functional groups. The unsaturations are of two basic types. Azomethine linkages (imine) not in conjugation with one another are referred to as isolated imine functions. Pairs of conjugated imine functions in the same five-membered chelate rings are referred to as α -diimine functions. One of the five remaining macrocyclic ligands, h, is very closely related to the majority of the structures but has a carbon skeleton which places *gem*-dimethyl groups *cis* to one another instead of in the *trans* position. Structure i represents a 14-membered ring similar to a but having only two methyl substituents, both located in one of the five-membered chelate rings. Structure j is a high-symmetry 16-membered ring which contains four imine functions. The reaction of complexes of this ligand (j) with NaOCH_3 generates the dianion k. A cyclic thioether (l) has also been included; it is the sulfur analog of a and i.

In the heme-proteins of natural systems the Möss-

bauer nucleus (iron) is at the functional site; thus, changes in Mössbauer spectral parameters may serve as a direct probe at the point of crucial interactions. Explaining the observed changes as a function of structure and bonding ability of the groups involved is not an easy matter. On the other hand, synthetic cyclic ligands provide ideal systems for studying these effects by Mössbauer spectroscopy, because an assortment of ring sizes, degrees of unsaturation, and net ligand charge are available. To contribute to the foundations required for understanding structure-function relationships in the natural systems, we have compared the Mössbauer parameters of these relatively simple synthetic systems with those of materials containing phthalocyanine and substituted porphyrins.

Theory

A useful demonstration of the manner in which the Mössbauer center shift¹² can be used to examine the bonding properties of a group of iron complexes has recently been reported.¹¹ It was shown that the total center shift (cs) of a series of six-coordinate, low-spin Fe(II) complexes may be treated as the sum of the individual contributions made by the six ligating groups,

$$cs = \sum_{i=1}^6 (pcs)_i \quad (1)$$

where pcs is the partial center shift ascribable to the *i*th ligand. The pcs values are easily calculated by dividing the cs values of certain octahedral complexes by six. The appropriate complexes are those having six identical donors. The pcs values thus obtained may be treated as characteristic constants for the particular ligands in question. Furthermore, the known pcs values can be used in mixed ligand complexes to derive pcs values of other ligands. For ⁵⁷Fe, the interaction between the nuclear quadrupole moment and the electric field gradient generated by the environment of the iron nucleus gives rise to a two-line spectrum, with the splitting ΔE_q given by

$$\Delta E_q = \frac{1}{2} e^2 q Q \left(1 + \frac{\eta^2}{3} \right)^{1/2} \quad (2)$$

where *e* is the electronic charge, *q* is the electric field gradient at the nucleus, *Q* is the quadrupole moment of the 14.37 keV nuclear state of ⁵⁷Fe, and η is the asymmetry parameter. The quantity *q* can be expressed as the sum of the two contributions

$$q = (1 - R)q_{\text{valence}} + (1 - \gamma_{\infty})q_{\text{lattice}} \quad (3)$$

where *R* and γ_{∞} are Sternheimer antishielding factors.¹³ The valence contribution is determined by the electron occupancy of the iron d orbitals, and the lattice contribution is related to the positions of external charges, such as ligands and ions in the crystal.

The contributions made to the total field gradient by the individual ligands can be summed as follows¹¹

$$q = \sum_{i=1}^6 (3 \cos^2 \theta - 1)_i [X]_i \quad (4)$$

(12) The center shift is the sum of the isomer shift and the second-order Doppler shift. For the present study the source and absorber are at the same temperature, so that the second-order Doppler term is approximately zero. In the following discussion the terms isomer shift and center shift will be used interchangeably: Y. Hazony, *J. Chem. Phys.*, **45**, 2664 (1966).

(13) J. O. Artman, A. H. Muir, Jr., and H. Weidersich, *Phys. Rev.*, **173**, 337 (1968).

In this expression θ is the angle between the *z* axis of the complex and the coordinated ligand, *X*, and $[X]_i$ is the contribution to *q* due to *X*. Assuming true octahedral angles and $\eta = 0$ for tetragonally distorted *trans*-FeA₂B₄ complexes, evaluation of eq 2 and 4 yields

$$\Delta E_q = +4(pqs)_A - 4(pqs)_B \quad (5)$$

Equation 5 introduces a new quantity, the partial quadrupole splitting (pqs). By choosing a reference value of -0.30 mm/sec for coordinated chloride and using the sign of the quadrupole splitting for several complexes, pqs values have been assigned to a large family of ligands.¹¹ The present studies provide an extensive demonstration of the generality of the treatment summarized above.

Results

Experimental Data. The Mössbauer center shift δ and splitting ΔE_q for the macrocyclic iron complexes are given in Table I. The complexes which the cyclic ligands form with iron can be conveniently divided into three groups on the basis of oxidation state, spin state, and coordination number. The six-coordinate diamagnetic complexes (*S* = 0) of divalent iron constitute the largest group. Their observed center shifts range from 0.21 to 0.63 mm/sec relative to stainless steel. In general, the shift decreases as the degree of unsaturation of the cyclic ligand increases. A similar decrease in shift is observed as the ligand field strength of the axial ligand increases. Thus for any given macrocyclic ligand the isomer shift decreases in the order SCN⁻ \approx CH₃CN \approx imidazole > NO₂⁻ > CN⁻. The quadrupole splitting ΔE_q varies from ~ 0 mm/sec for the [14]janeS₄ complex (Figure 1, ligand 1) to 1.86 mm/sec for the complex with [14]1,3,7,11-tetraeneN₄. The shifts for the iron(II) complexes containing four unpaired electrons (*S* = 2) are all greater than 0.90 mm/sec, with quadrupole splittings up to 4.07 mm/sec.

Five six-coordinate, tetragonally distorted, low-spin iron(III) complexes have been examined. These compounds have relatively large quadrupole splittings (1.46–2.72 mm/sec) compared with high-spin iron(III) systems which usually have values under 1.0 mm/sec; their isomer shifts show a small variation and range from 0.21 to 0.32 mm/sec. The two iron(III) complexes involving the TAAB ligand exist as μ -oxo bridged dimers and are five-coordinate; these materials exhibit anomalous moments at room temperature as a result of antiferromagnetic coupling through the oxygen bridge of the two *S* = $5/2$ iron atoms. The ΔE_q values of these bridged compounds are relatively small, 0.83 and 1.05 mm/sec, consistent with a ⁶A ground state;¹⁴ the isomer shifts are slightly higher than those usually recorded for low-spin Fe(III) complexes.

Partial Center Shifts for Low-Spin Iron(II) Complexes. All of the complexes in this group contain a cyclic tetradentate ligand in the plane and two identical monodentate ligands in the axial sites. We have assumed that the six donor atoms lie on mutually orthogonal axes as in a true octahedron, but the following caution must be noted with respect to the macrocycles. Single-crystal X-ray analyses of metal complexes containing ligands similar to [14]janeN₄¹⁵ and [14]4,11-

(14) I. A. Cohen, *J. Amer. Chem. Soc.*, **91**, 1980 (1969).

(15) B. Bosnich, R. Mason, P. J. Pauling, G. B. Robertson, and M. L. Tobe, *Chem. Commun.*, 97 (1965).

Table I. Mössbauer Parameters for Some Iron Complexes with Macrocyclic Ligands^a

Compd no.	Complex	$\delta,^b$ mm/sec	$\Delta E_q,^c$ mm/sec
Low-Spin Fe(II) ($S = 0$)			
1	Fe([14]aneN ₄)(SCN) ₂	0.63 (-0.02)	(+)0.29 ^d
2	[Fe([14]aneN ₄)(CH ₃ CN) ₂](ClO ₄) ₂ ^e	0.60 (0)	(+)0.55 ^d
3	Fe([14]aneN ₄)(NO ₂) ₂	0.54 (0)	0.75 ^f
4	Fe([14]aneN ₄)(CN) ₂ ^g	0.43 (0)	(-)1.10 (0)
5	[Fe(Me ₂ [14]aneN ₄)(CH ₃ CN) ₂](ClO ₄) ₂	0.56	(+)0.65 (-0.01)
6	Fe([14]4,11-dieneN ₄)(SCN) ₂	0.54 (-0.01)	(+)0.77 (-0.03)
7	[Fe([14]4,11-dieneN ₄)(Im) ₂](BPh ₄) ₂	0.52 (+0.01)	(+)1.07 (-0.23)
8	[Fe([14]4,11-dieneN ₄)(CH ₃ CN) ₂](ClO ₄) ₂	0.51 (+0.01)	(+)1.07 (-0.07)
9	Fe([14]4,11-dieneN ₄)(CN) ₂	0.36 (-0.01)	(-)0.70 (-0.04)
10	[Fe([14]1,4,4,11-trieneN ₄)(CH ₃ CN) ₂](ClO ₄) ₂	0.47 (0)	(+)1.28 (-0.05)
11	Fe([14]1,4,8,11-tetraeneN ₄)(SCN) ₂	0.44 (0)	(+)1.21 ^d
12	[Fe([14]1,4,8,11-tetraeneN ₄)(Im) ₂](BF ₄) ₂	0.45 (-0.01)	(+)1.30 ^d
13	[Fe([14]1,4,8,11-tetraeneN ₄)(CH ₃ CN) ₂](ClO ₄) ₂	0.44 (-0.01)	(+)1.36 (+0.10)
14	Fe([14]1,4,8,11-tetraeneN ₄)(NO ₂) ₂	0.36 (+0.01)	(+)1.08 ^d
15	[Fe(TAAB)(CH ₃ CN) ₂](ClO ₄) ₂	0.47	(+)0.82 ^d
16	[Fe([14]1,3,8-trieneN ₄)(SCN) ₂]	0.40 (+0.05)	(+)1.35 (-0.24)
17	[Fe([14]1,3,8-trieneN ₄)(Im) ₂](BF ₄) ₂	0.41 (+0.04)	(+)1.50 (-0.29)
18	[Fe([14]1,3,8-trieneN ₄)(CH ₃ CN) ₂](PF ₆) ₂	0.41 (+0.03)	(+)1.23 (+0.14)
19	Fe([14]1,3,8-trieneN ₄)(CN) ₂	0.21 (+0.06)	0.90 ^f
20	[Fe([14]1,3,7,10-tetraeneN ₄)(CH ₃ CN) ₂](PF ₆) ₂	0.39 (+0.01)	(+)1.51 (+0.09)
21	[Fe([14]1,3,7,11-tetraeneN ₄)(CH ₃ CN) ₂](BPh ₄) ₂	0.40 (0)	(+)1.86 (-0.26)
22	Fe([14]1,3,8,10-tetraeneN ₄)(SCN) ₂	0.36 (+0.02)	(+)1.49 ^d
23	[Fe([14]1,3,8,10-tetraeneN ₄)(CH ₃ CN) ₂](PF ₆) ₂	0.40 (-0.03)	(+)1.41 (+0.33)
24	Fe([14]1,3,8,10-tetraeneN ₄)(NO ₂) ₂	0.32 (-0.01)	(+)1.39 (-0.03)
25	Fe([14]1,3,8,10-tetraeneN ₄)(CN) ₂	0.21 (-0.01)	1.09 ^f
26	[Fe([14]aneS ₄)(CH ₃ CN) ₂](BF ₄) ₂	0.48	~0 ^d
High-Spin Fe(II) ($S = 2$)			
27	Fe([14]aneN ₄)(I) ₂	0.96	1.28
28	Fe([14]aneN ₄)(Br) ₂	0.93	1.73
29	Fe([14]aneN ₄)(Cl) ₂	1.01	2.11
30	Fe([14]aneN ₄)(CH ₃ CO ₂) ₂	1.07	4.07
Low-Spin Fe(III) ($S = 1/2$)			
31	[Fe(Me ₂ [14]aneN ₄)(CH ₃ CN) ₂](ClO ₄) ₃	0.24	1.77
32	[Fe([14]4,11-dieneN ₄)(Cl) ₂](ClO ₄)	0.32	2.66
33	[Fe([14]4,11-dieneN ₄)(NCS) ₂]BPh ₄	0.26	2.18
34	[Fe([14]1,3,8-trieneN ₄)(Cl) ₂]PF ₆	0.25	2.62
35	[Fe([14]1,3,8,10-tetraeneN ₄)(Cl) ₂]PF ₆	0.21	2.72
μ -Oxo Bridged Dimeric Complexes Fe(III) ($S = 5/2$)			
36	[Fe(TAAB)] ₂ O(BPh ₄) ₂	0.43	0.83
37	[Fe(TAAB)(OMe) ₂]O	0.37	1.05

^a Data obtained at 298°K. For the structures of the cyclic ligands see Figure 1. Abbreviation: Im, imidazole. ^b The shift relative to stainless steel is given, followed by the quantity ($\delta_{\text{calcd}} - \delta_{\text{obsd}}$). δ_{calcd} is calculated as outlined in the text. ^c The inferred sign and magnitude of the quadrupole splitting is given, followed by the quantity ($\Delta E_{q(\text{calcd})} - \Delta E_{q(\text{obsd})}$). $\Delta E_{q(\text{calcd})}$ is obtained as outlined in the text. ^d Compound used to calculate a ligand pqs value. ^e Contains 1.5CH₃CN of crystallization. ^f Sign of ΔE_q uncertain. ^g Contains 2H₂O of crystallization.

dieneN₄¹⁶ have shown that the N-M-N (M = metal) bond angles are smaller for the five-membered chelate ring (86°) than the corresponding angle for the six-membered ring (94°). This kind of distortion is expected to be relatively large for a structure such as [14]1,3,8,10-tetraeneN₄. However, X-ray data show that the central metal ion and the donors lie close to one plane, and, in the following discussion, D_{4h} symmetry will be assumed.

The center shift for the six-coordinate diamagnetic complexes can be placed on a quantitative basis using the concept of the partial center shift. Since octahedral complexes containing these tetradentate macrocycles (MAC) as the sole ligands do not exist, the center shift values of Fe(MAC)X₂, where X⁻ = CN⁻ or NO₂⁻, were used to establish the pcs values of the macrocyclic ligands. The cs values of hexanitro and hexacyano complexes, K₂CaFe(NO₂)₆^{17,18} and K₄Fe(CN)₆,¹⁸

are +0.39 and +0.05 mm/sec, respectively, resulting in pcs values of 0.065 and 0.009 mm/sec for NO₂⁻ and CN⁻ (Table II). For the macrocycles (Figure 1) [14]aneN₄, [14]1,4,8,11-tetraeneN₄, and [14]1,3,8,10-tetraeneN₄, a CN⁻ and/or NO₂⁻ derivative exists, and this allows the direct determination (eq 1) of the pcs values of the macrocycles. Having established these pcs values, those for the remaining ligands were calculated.

It was also possible to divide pcs values of the macrocyclic ligands into the contributions made by individual functional groups, and these are also listed in Table II. The spectral properties of [14]aneN₄ and Me₂[14]aneN₄ show them to have different ligand field strengths,¹⁹ and they have been considered separately. The agreement between the observed and calculated isomer shift values is shown in Figure 2 and presented numerically in Table I. A linear regression analysis gives a correlation coefficient of 0.98 with a slope of 0.93 ± 0.05 and intercept of 0.04 ± 0.02 . The greatest dis-

(16) B. T. Kilbourn, R. R. Ryan, and J. D. Dunitz, *J. Chem. Soc. A*, 2407 (1969), and references therein.

(17) H. Sano and H. Kono, *Bull. Chem. Soc. Jap.*, **38**, 1228 (1965).

(18) E. Fluck and P. Kuhn, *Z. Anorg. Allg. Chem.*, **350**, 263 (1967).

(19) E. S. Gore, J. C. Dabrowiak, and D. H. Busch, *J. Chem. Soc., Chem. Commun.*, 923 (1972).

Table II. Partial Center Shifts for Some Ligands Bound to Low-Spin Fe(II)^a

Ligand ^b	Pcs, mm/sec
[14]aneN ₄ /4 (R ₂ NH)	0.103
Imidazole	0.100, 0.08 ^c
SCN ⁻	0.100, 0.05 ^c
Me ₂ [14]aneN ₄ /4 (R ₂ NH)	0.095
CH ₃ CN	0.093 ^d
S—	0.073 ^d
TAAB N=C	0.070 ^d
NO ₂ ⁻	0.065, 0.05 ^c
Isolated, R—N=C	0.060
α, R—N=C	0.045
CN ⁻	0.009, 0.01 ^c

^a All values calculated relative to stainless steel. The pcs values of the macrocycle are per functional group of the cyclic ligand. ^b Abbreviation: isolated and α-RN=C are as described in the text. ^c From ref 11. ^d Based on the trans acetonitrile.

crepancy between observed and calculated values occurs for the complexes with [14]1,3,8-trieneN₄. This is not surprising since this system provides the most stringent test of the additive nature of the pcs values. Changes in bond distances and angles must affect the pcs values; this should limit their additivity.

Partial Quadrupole Splitting Values for Low-Spin Iron(II) Complexes. In order to determine pqs values for the axial and macrocyclic ligands the sign of ΔE_q for the complexes must be determined. Since neither single-crystal nor magnetic Mössbauer studies have been conducted on these complexes, some of the pqs values determined in an earlier study were used as reference values.²⁰ Ligands common to both studies and for which accurate pqs values are available are CN⁻, SCN⁻, and NH₃, the latter being very similar to a secondary amine (e.g., [14]aneN₄, Me₂[14]aneN₄). By considering the observed quadrupole splitting for Fe([14]aneN₄)(SCN)₂ and Fe([14]aneN₄)(CN)₂, along with the pqs values of CN⁻ (-0.84 mm/sec), SCN⁻ (-0.49 mm/sec), and NH₃ (-0.51 mm/sec), it was concluded that the signs of ΔE_q for the two complexes are positive and negative, respectively. This assumption and the great similarity between all of the structures, particularly with regard to donor atoms, has allowed us to predict the signs of the quadrupole splittings for all but three of the complexes shown in Table I.

Of the 26 structures studied, eight were used to determine the pqs values of the various functional groups present in the complexes. The values obtained for the macrocyclic ligands were divided by four to get the pqs values of the individual functional groups. These values were then used with the expressions shown in Table III to calculate the ΔE_q values of the complexes. As an example, the ΔE_q of *trans*-Fe([14]1,3,8-trieneN₄)(CH₃CN)₂²⁺ has the following form.

$$\Delta E_q = 4(\text{pqs CH}_3\text{CN}) - (\text{pqs R}_2\text{NH}) - (\text{pqs RN}=\text{C}) - 2(\text{pqs } \alpha \text{ RN}=\text{C}) \quad (6)$$

(20) G. M. Bancroft, R. E. B. Garrod, and A. G. Maddock, *J. Chem. Soc. A*, 3165 (1971).

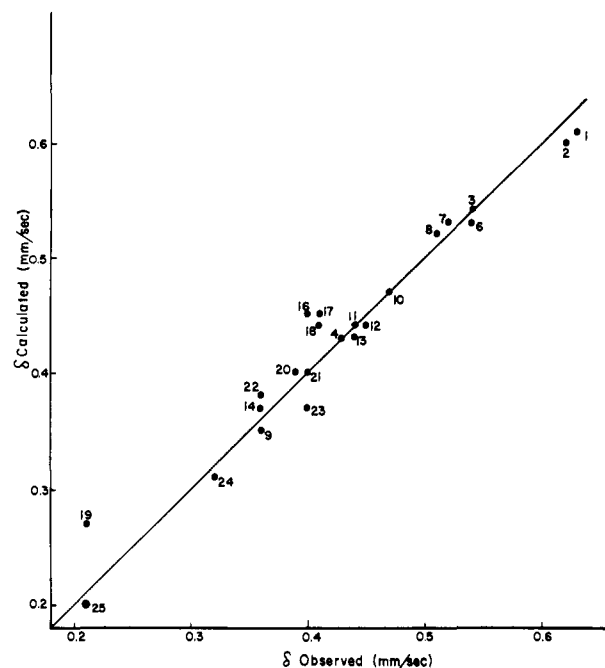


Figure 2. Graph showing the agreement between δ calculated and δ observed for some low-spin iron(II) macrocyclic complexes. The numbers in the figure refer to Table I.

Table III. Macrocyclic Contributions to Quadrupole Splitting

Macrocycle	Contribution to $\Delta E_q(\text{total})^{\text{a}, \text{c}}$	η^{b}
[14]aneN ₄	-4[A]	0
Me ₂ [14]aneN ₄	-4[A]	0
[14]4,11-dieneN ₄	-2[A] - 2[B]	>0
[14]1,4,11-trieneN ₄	-[A] - 3[B]	>0
[14]1,4,8,11-tetraeneN ₄	-4[B]	0
[14]1,3,8-trieneN ₄	-[A] - [B] - 2[C]	>0
[14]1,3,8,10-tetraeneN ₄	-4[C]	0
[14]1,3,7,10-tetraeneN ₄	-2[B] - 2[C]	>0
[14]1,3,7,11-tetraeneN ₄	-2[B] - 2[C]	>0
TAAB	-4[D]	0
[14]aneS ₄	-4[E]	0

^a Calculated using eq 4 in the text. ^b The asymmetry factor η , eq 2 of text. ^c Functional groups: A, NHR₂; B, isolated RN=C; C, α-RN=C; D, N=C; E, SR₂.

Table IV. Partial Quadrupole Splittings for Some Ligands Bound to Low-Spin Fe(II)

Ligand ^a	pqs, mm/sec	Ligand ^a	pqs, mm/sec
α, R—N=C	-0.86	NO ₂ ⁻	-0.52
CN ⁻	-0.84 ^b	SCN ⁻	-0.49 ^b
Isolated, R—N=C	-0.79	Imidazole	-0.46
TAAB, N=C	-0.62	CH ₃ CN	-0.42, -0.43 ^c
R ₂ NH	-0.56	SR ₂	-0.42

^a Abbreviation: isolated and α-RN=C are as described in the text. ^b From ref 20. ^c Calculated from *trans*-[Fe(H)(CH₂CN)(depe)₂]BPh₄ as given by G. M. Bancroft, R. E. B. Garrod, A. G. Maddock, M. J. Mays, and B. E. Prater, *J. Amer. Chem. Soc.*, **94**, 647 (1972).

Table IV lists the pqs values calculated from eq 5 for the functional groups contained in the cyclic ligands. The agreement between observed and calculated ΔE_q

Table V. Linear Regression Analysis of the Correlations

Plot ^a	No. of points	Slope ^b	Intercept ^c	Correlation coefficient
pcs(X), Fe(II) vs. Dq_x , Co(III)	11	$-12 (\pm 3) \times 10^3$	$3.4 (\pm 0.2) \times 10^3$	-0.81
pcs(X), Fe(II) vs. Dq_x , Ni(II)	6	$-10 (\pm 4) \times 10^3$	$2.2 (\pm 0.3) \times 10^3$	-0.78
pqs(X), Fe(II) vs. Dq_x , Co(III)	10	$-2.3 (\pm 0.5) \times 10^3$	$1.2 (\pm 0.3) \times 10^3$	-0.87
pqs(X), Fe(II) vs. Dq_x , Ni(II)	5	$-2.0 (\pm 0.6) \times 10^3$	$0.12 (\pm 0.4) \times 10^3$	-0.89
ΔE_q , Fe(II) vs. $(Dq_{xy} - Dq_x)$, Co(III)	20	$5.5 (\pm 0.7) \times 10^2$	$0.8 (\pm 0.8) \times 10^2$	+0.88
δ , Fe(II) vs. $\nu(A_{1g} \rightarrow T_{1g})$ Fe(II)	8	$-1.4 (\pm 0.3) \times 10^4$	$2.6 (\pm 0.2) \times 10^4$	-0.88
pcs (MAC) vs. $\nu(C \equiv N)$	4	$0.20 (\pm 0.04) \times 10^3$	$2.02 (\pm 0.01) \times 10^3$	+0.99
δ vs. ΔE_q (CH_3CN complexes)	7	$-4.0 (\pm 0.16)^d$	$3.1 (\pm 0.3)^e$	-0.95

^a See text for description of plot. X refers to the ligands listed in Tables II and IV. ^b Units are $cm^{-1} mm^{-1} sec$ unless otherwise noted. ^c Units in cm^{-1} unless otherwise noted. ^d Unitless. ^e Units: mm/sec.

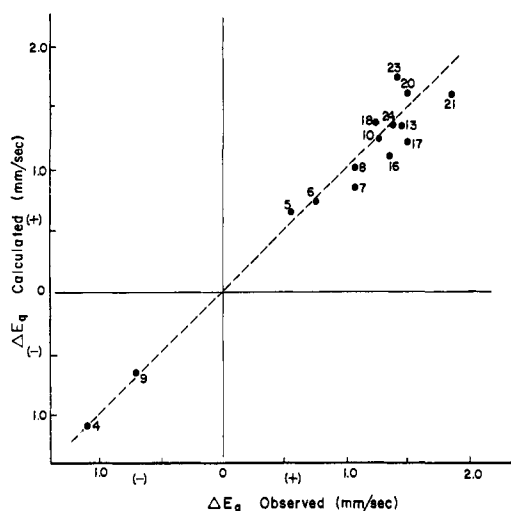


Figure 3. Graph showing the agreement between ΔE_q calculated and ΔE_q observed for some low-spin iron(II) macrocyclic complexes. The numbers in the figure refer to Table I.

is shown in Table I and Figure 3. A linear regression analysis of the data shown in Figure 3 gives a slope of 0.97 ± 0.06 with an intercept of -0.01 ± 0.07 and a correlation coefficient of 0.98. The agreement between the calculated values of 15 of the 18 complexes not used as standards is within ± 0.3 mm/sec of the observed value, with most much better than this limit. For $Fe([14]1,3,8\text{-trien}N_4)(CN)_2$, $Fe([14]1,3,8,10\text{-tetra}eneN_4)(CN)_2$, and $Fe([14]aneN_4)(NO_2)_2$ the agreement is poor, and data for these compounds were not used in constructing the correlation plot shown in Figure 3. For these complexes even the sign of ΔE_q is difficult to predict; indeed, assignment of either positive or negative signs for these structures does not help the agreement. For these three materials the syntheses and measurements were repeated, with no change in the experimental results. The anomalous splittings suggest that the three compounds differ from the others and have unusual structural features that are not fully understood.

The agreement between observed and calculated ΔE_q values is remarkable in view of the sensitivity of the quadrupole splitting to a variety of factors. The presence of other ions in the unit cell not directly bound to the Mössbauer nuclide is known to affect the quadrupole splittings.²¹ Due to the difficulty in isolation and characterization of many of the desired materials,

(21) E. Fluck, "Chemical Applications of Mössbauer Spectroscopy," V. I. Goldanski and R. H. Herber, Ed., Academic Press, New York, N. Y., 1968, p 268.

consistency with regard to the counterion was not possible. Thus, for the *trans*- CH_3CN and imidazole complexes the noncoordinating anions, ClO_4^- , BF_4^- , PF_6^- , and BPh_4^- were employed. An illustration of the effects of such lattice contributions was provided by $Fe([14]1,4,8,11\text{-tetra}eneN_4)(CH_3CN)_2^{2+}$ which was isolated as both the ClO_4^- and BPh_4^- salts. The measured values of ΔE_q were 1.36 and 1.50 mm/sec, respectively, for the two complexes. This difference is probably due to the different relative spatial arrangement of the anions in the unit cell or to possible steric effects the large BPh_4^- ion might impose on the groups involved in the primary coordination sphere of the metal. Other possible sources of error are the assumed invariance of the pqs values and the value of η assumed in calculations for some of the complexes (Table III). Discrepancies caused by the asymmetry parameter should be small since the full range of values of $(1 + \eta^2/3)^{1/2}$ (eq 2) is from 1.00 to 1.16.

Discussion

The Low-Spin Iron(II) Complexes. The partial center shifts and partial quadrupole splittings derived here can be used to infer certain relationships involving the electronic structures and bonding among these complexes.

The center shift is directly related to the s-electron density at the nucleus; ligands that are good σ donors and those that are good π acceptors will cause an increase in this s-electron density. The importance of π -bonding ability can readily be demonstrated by considering the shielding effects of the t_{2g} electrons for low-spin iron(II). Ligands which are able to π bond with the filled t_{2g} orbitals will withdraw electron density from these orbitals, leading to a decrease in the shielding of the 3s and 4s electrons. Direct σ donation will also lead to increased s density at the nucleus, and both factors result in a decrease in the center shift.

The d-d electronic transitions for many of the Fe(II) macrocyclic complexes are obscured by charge transfer transitions. This limits the use of uv-visible absorption spectroscopy in the determination of ligand field strengths.²² Following the notion that ligand field effects are directly related to pcs and pqs values, we have plotted the Dq values of the ligand, as determined from cobalt(III)^{14, 23-25} and nickel(II)²⁶ complexes, against the Mössbauer parameter (Table V). In

(22) P. Krumholz, *Struct. Bonding (Berlin)*, **9**, 139 (1971).

(23) A. M. Tait and D. H. Busch, to be submitted for publication.

(24) S. C. Cummings and D. H. Busch, *Inorg. Chem.*, **10**, 1220 (1971).

(25) R. A. D. Wentworth and T. S. Piper, *Inorg. Chem.*, **4**, 709 (1965).

(26) C. R. Sperati, Thesis, The Ohio State University, 1970.

general the correlation is good, yielding correlation coefficients of -0.78 to -0.89 . The pcs values are four to five times more sensitive to changes in ligand field strength than are the pqs values. This is due to the fact that σ - and π -bonding effects act in the same direction in affecting the cs but act in opposition in affecting ΔE_q .¹¹ Thus the synergistic effect of the π back-bonding on the strengths of σ bonds is seen most sharply in the center shift values.

Assuming that bond moments are proportional to ligand fields it is also possible to correlate the difference between the ligand field in the xy plane (macrocyclic ligand) and the field in the z direction (axial ligands) with ΔE_q . If the field gradient at the nucleus is dominated by the six coordinating groups, the electronic spectral parameters should provide a measure of this gradient. Taking into consideration that electronic data from cobalt(III) are employed,²² the correlation between ΔE_q for the iron(II) complexes and $(Dq_{xy} - Dq_z)$ shown in Table V is remarkable.

The $\text{Fe}([\text{14}] \text{janeS}_4)(\text{CH}_3\text{CN})_2^{2+}$ complex shows no measurable ΔE_q implying that the field gradient produced by the four thioether functional groups and the two nitrile ligands vanishes. The cobalt(III) data for this system suggest the presence of a small tetragonal splitting, with $(Dq_{xy} - Dq_z) \sim 300 \text{ cm}^{-1}$.^{14,23} However, such a small splitting cannot be observed directly in the visible spectra, and less direct methods must be employed in evaluating the quantity $(Dq_{xy} - Dq_z)$.²⁵

For a few of the iron(II) complexes a direct correlation can be attempted between ligand field strengths,²⁻⁴ as measured spectroscopically on low-spin iron(II) complexes, and the isomer shift (Figure 4). The electronic spectra contain distinct bands assignable to d-d transitions in certain of these complexes (when there are no α -diimine functions in the macrocyclic ligand). The positions of the Gaussian-shaped low-energy bands are directly related to the average ligand field strengths of the complexes. Assuming octahedral symmetry, the actual band position is $10Dq - C(A_{1g} \rightarrow T_{1g})$, and the Racah parameter C is relatively constant.⁴ The correlation shown in Table V and Figure 4 makes possible the estimation of ligand field strengths for iron complexes for which the pertinent electronic spectral bands are not directly observed, e.g., derivatives of macrocycles containing α -diimine functions. From the cs values listed in Table I, $[\text{14}]\text{1,3,8,10-tetraeneN}_4$ produces the strongest ligand field from among the macrocycles. Using the parameters in Table V, an $A_{1g} \rightarrow T_{1g} (O_h)$ transition should appear at $\sim 20.5 \text{ kK}$. Direct observation of this band is not possible because of intense charge transfer bands which occur in this region.⁵ Assuming C to be $\sim 3.3 \text{ kK}$, Dq_{xy} is about 2400 cm^{-1} , considerably higher than the ligand field strength estimated for $\text{Fe}(\text{bipy})_3^{2+}$ which also contains α -diimine functions. The ligand field strength of 2,2'-bipyridine toward low-spin Fe(II) may be inferred from a comparison of the cs values of the macrocyclic complexes with those of a series of iron(II) bipy complexes;¹¹ the value obtained is close to 2400 cm^{-1} , rather than $1650\text{--}1900 \text{ cm}^{-1}$ as other workers have suggested.²⁷

Table II shows that the order of pcs values is $\text{CN}^- < \alpha$ -diimine $<$ isolated imine $<$ $\text{NO}_2^- <$ $\text{SR}_2 <$ $\text{CH}_3\text{CN} <$

(27) R. A. Palmer and T. S. Piper, *Inorg. Chem.*, **5**, 864 (1966).

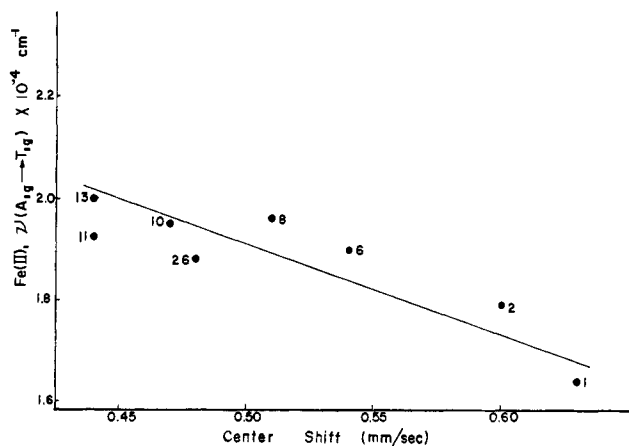
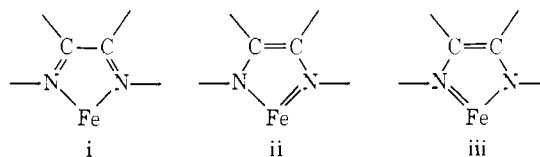


Figure 4. Correlation between the center shift and the $A_{1g} \rightarrow T_{1g} (O_h)$ transition for some low-spin Fe(II) macrocyclic complexes. The numbers in the figure refer to Table I.

imidazole $\approx \text{SCN}^- <$ NHR_2 . From this order it is evident that increasing the unsaturation in the macrocycle lowers the center shift. The pcs value of NHR_2 is greater than the pcs value of the isolated imine which, in turn, is greater than that of the α -diimine. The most likely reason for this is the increase in π accepting power of the in-plane ligand. Investigations on the cyanide stretching frequencies in the infrared spectra of $\text{Fe}([\text{14}] \text{janeN}_4)(\text{CN})_2$, $\text{Fe}([\text{14}]\text{4,11-dieneN}_4)(\text{CN})_2$, $\text{Fe}([\text{14}]\text{1,3,8-trieneN}_4)(\text{CN})_2$, and $\text{Fe}([\text{14}]\text{1,3,8,10-tetraeneN}_4)(\text{CN})_2$ show small but measurable changes in the sharp singlet. This absorption for the above complexes occurs at 2054 , 2071 , 2094 , and 2099 cm^{-1} , respectively, and varies linearly with the pcs values of the macrocycles (Table V); the correlation is excellent. This kind of behavior can be attributed to the removal of electron density from the d_{zz} and d_{yz} orbitals of the metal by the imine functions. This decreases the electron density in antibonding π orbitals on the axial cyanide ligands. The carbon-nitrogen bond of the CN^- is strengthened, and its stretching mode shifts to higher energy.

The pcs value of the α -diimine function (0.045 mm/sec) is very similar to that reported for some bidentate phosphine ligands.¹¹ This notable coincidence of pcs values for these two functional groups supports the point of view that both are good π acceptors. π interactions in Fe α -diimine complexes are generally ascribed to the large contribution of resonance structures ii and iii below. That these contributions are significant is sup-



ported by infrared²⁸ and visible absorption data²² on the Fe(II) complexes containing this functional unit.

The importance of π bonding in these macrocyclic complexes can be further demonstrated by the plot of cs vs. ΔE_q shown in Figure 5. Since the cs is dependent on the sum of σ and π bonding ability of the ligands and

(28) D. H. Busch and J. C. Bailar, Jr., *J. Amer. Chem. Soc.*, **78**, 1137 (1956); K. Nakamoto, "Advances in the Chemistry of the Coordination Compounds," S. Kirschner, Ed., Macmillan, New York, N. Y., 1961, p 437.

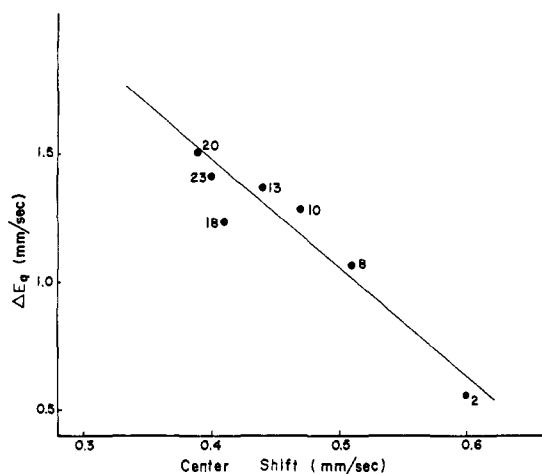


Figure 5. Correlation between the center shift and ΔE_q for some low-spin Fe(II) macrocyclic complexes. The numbers in the figure refer to Table I.

ΔE_q depends on the difference between these effects,¹¹ a linear relationship between these two Mössbauer parameters for a given series of complexes implies that one of the effects changes relatively little in the series.²⁹ Hence for a group of ligands which are essentially σ donors a plot of *cs* vs. ΔE_q has a positive slope.³⁰ If π effects predominate the slope is expected to be negative as is the case shown in Figure 5. For this analysis complexes with trans acetonitrile groups and cyclic ligands having the same basic carbon skeleton but different positions and degrees of unsaturation were chosen. The observed negative slope must be due to the enhanced π bonding ability of the imine functional groups, further supporting the previously mentioned conclusions.

The Paramagnetic Iron Complexes. The remaining paramagnetic complexes can be separated into two groups according to oxidation state. Four of these materials contain six-coordinate, high-spin ($S = 2$) iron(II) and the [14]aneN₄ macrocycle (Table I). Although there are too few complexes to draw any firm conclusions, the *cs* and ΔE_q values appear to be related to the electronegativities of the axial ligands.³¹ The calculated electronegativities for I, Br, Cl, and O are 2.2, 2.7, 2.8, and 3.5, respectively.³² Evidence that the isomer shift for such systems may also be related to the nephelauxetic effect has previously been forwarded.³³

The visible absorption data for these compounds⁴ show that the ligand field on the *z* axis is weaker than the in-plane field but that the acetate complex is closest to being octahedral in symmetry (*i.e.*, shows the least lower-symmetry splitting). The trend of ΔE_q values observed in the high-spin Fe(II) macrocycles is supported by ΔE_q values for Fe(H₂O)₆SiF₆ (3.5 mm/sec) and *trans*-Fe(H₂O)₄Cl₂ (3.0 mm/sec),³⁰ and the fact that $Dq(\text{Cl}^-)$ is less than $Dq(\text{H}_2\text{O})$.³⁴ The differ-

ence in strength between the in-plane and out-of-plane fields is greatest for the trans dichloro complexes, which also have the smaller ΔE_q values. These observations are also consistent with q_{lattice} effects being opposite in sign to q_{valence} . Thus q_{lattice} is nearest to zero for the acetate complex giving $\Delta E_q \sim q_{\text{valence}}$. As the axial ligand field strength decreases from acetate to iodide the absolute value of q_{lattice} increases and that of ΔE_q decreases.

The low-spin six-coordinate Fe(III) derivatives have magnetic moments consistent with one unpaired electron ($S = 1/2$). Only five derivatives are presented, but it appears that the isomer shift is sensitive to changes in macrocyclic structure. For the trans dichloro complexes, increasing the degree of unsaturation in the macrocycle lowers the isomer shift. A comparison of the iron(II) and -(III) NCS⁻ derivatives of [14]4,11-dieneN₄ shows that the effect of one less d electron on the isomer shift is dramatic. Since the d electrons shield the nucleus from s density a decrease in their number should lower the isomer shift. In this case the magnitude is 0.2–0.3 mm/sec, which is similar to that observed for the iron(II) and -(III) tris(1,10-phenanthroline) and bipyridyl complexes.³³ The effects of π bonding on the isomer shift as a function of axial ligand can be found in the Cl⁻ and SCN⁻ derivatives of Fe([14]4,11-dieneN₄).² The σ -donating and π -accepting abilities of Cl⁻ are poorer than those of SCN⁻, and the halide has the highest *cs* value. Although the *cs* values for these complexes may be explained using the concept of partial center shift, it is tenuous to do so until more derivatives are at hand.

The μ -oxo bridged dimers are included in Table I. The magnetic data for these materials show them to contain two ⁵⁷Fe iron(III) atoms involved in spin-spin coupling through the oxygen bridge.⁶ The resulting moments at room temperature are 1.9–2.2 BM, and their magnitudes are strongly temperature dependent. It is suggested that the two examples reported are both five coordinate and probably have the iron atom raised out of the plane of the cyclic ligand. X-Ray analysis of similar porphyrin complexes has shown this to be the case.³⁵

Comparison with Other Cyclic Structures. The preceding discussion dealt with derivatives of ligands having relatively simple cyclic structures. Many of these materials have been subjected to detailed chemical and physical study. A search of the literature shows that a large number of complicated structures also contain cyclic ligands (heme iron), and pertinent Mössbauer parameters for some of these low-spin iron(II) complexes are collected in Table VI. These examples contain six-coordinate iron with identical ligands in the axial sites. Since it is not always possible to determine spin state, oxidation state, and coordination numbers using Mössbauer spectroscopy alone, supporting data such as elemental analysis, magnetic susceptibility, and conductance information were also sought in support of the examples chosen for this tabulation. Caution must be exercised in interpreting the *cs* values in a quantitative manner since the limits of error on the experiments differ from case to case. This problem is exemplified by the two independent determinations

(29) B. W. Dale, R. J. P. Williams, P. R. Edwards, and C. E. Johnson, *Trans. Faraday Soc.*, **64**, 620 (1968).

(30) Y. Hazony, R. C. Axtmann, and J. W. Hurley, Jr., *Chem. Phys. Lett.*, **2**, 440 (1968).

(31) K. Ono, A. Ito, and E. Hirahara, *J. Phys. Soc. Jap.*, **17**, 1615 (1962).

(32) F. A. Cotton and G. Wilkinson, "Advanced Inorganic Chemistry," Wiley, New York, N. Y., 1962, p 92.

(33) R. L. Collins, R. Pettit, and W. A. Baker, Jr., *J. Inorg. Nucl. Chem.*, **28**, 1001 (1966).

(34) M. A. Robinson, J. D. Curry, and D. H. Busch, *Inorg. Chem.*, **2**, 1178 (1963).

(35) E. B. Fleischer, *Accounts Chem. Res.*, **3**, 105 (1970).

Table VI. Mössbauer Parameters for Some Porphyrin and Phthalocyanine Six-Coordinate Iron(II) Complexes

Compound ^a	Ref	Temp, °K	δ , ^b mm/sec	ΔE_q , mm/sec
Fe(TPP)(Py) ₂	<i>c</i>	300	0.46	1.22
	<i>c</i>	77	0.51	1.15
	<i>d</i>	Room	0.50	1.18
	<i>d</i>	77	0.56	1.17
Fe(TPP)(Im) ₂	<i>d</i>	77	0.56	1.06
	<i>d</i>	Room	0.53	1.42
Fe(TPP)(Pip) ₂	<i>d</i>	77	0.59	1.42
	<i>d</i>	77	0.56	1.21
Fe(PP)(Py) ₂	<i>d</i>	77	0.53	0.95
	<i>d</i>	Room	0.53	1.43
Fe(PP)(Im) ₂	<i>d</i>	77	0.60	1.42
	<i>d</i>	77	0.37	2.05
Fe(Pc)(Py) ₂	<i>e</i>	295	0.46	1.89
	<i>e</i>	77	0.36	2.02
	<i>f</i>	293	0.36	2.02
	<i>f</i>	77	0.43	1.97
Fe(Pc)(Im) ₂	<i>e</i>	295	0.38	1.79
	<i>e</i>	77	0.47	1.71
	<i>f</i>	77	0.39	1.75
Fe(Pc)(Pip) ₂	<i>f</i>	77	0.43	2.21
Fe(Pc)(BAm) ₂	<i>f</i>	77	0.44	1.94

^a Abbreviations: TPP, $\alpha,\beta,\gamma,\delta$ -tetraphenylporphyrin; PP, protoporphyrin; Pc, phthalocyanine; Py, pyridine; Im, imidazole; Pip, piperidine; BAm, butylamine. ^b Shifts relative to stainless steel. ^c H. Kobayashi, Y. Maeda, and Y. Yanagawa, *Bull. Chem. Soc. Jap.*, **43**, 2342 (1970). ^d Reference 38. ^e Reference 36. ^f Reference 29.

of the *cs* values for the low spin bispyridine and bisimidazole phthalocyanine complexes as tabulated.^{29,36}

In view of the correlation between ligand field strengths and the *cs* values for iron(II) macrocyclic complexes, it may be possible to estimate the ligand field strengths of some porphyrin derivatives from their Mössbauer parameters. The porphyrin-imidazole complexes listed in Table VI have *cs* values which are significantly greater than those of the [SCN⁻] complex with the 14-membered macrocyclic ligand [14]1,3,8,10-tetraeneN₄. (Imidazole and SCN⁻ have identical *pcs* values.) It follows that the ligand field of the porphyrins should be less than that attributed to [14]1,3,8,10-tetraeneN₄ (>2400 cm⁻¹). This is not surprising since the porphyrin ring contains 16 members and probably has greater Fe-N distances than do most of the complexes reported here.⁵

A second apparent point of difficulty may also be explained by macrocycle ring-size effects. The electric field gradient was reported to be positive for bis(pyridine)phthalocyanineiron(II) ion.³⁷ This indicates that *Dq* for pyridine is less than *Dq* for phthalocyanine. Assuming ΔE_q is positive for the other phthalocyanine complexes, Table VI shows that imidazole is a stronger ligand than the secondary amine piperidine. However, Table IV shows that the opposite is true for the macrocycle data presented here—secondary amines (in 14-membered rings) are stronger donors than imidazole. The simplest rationalization of this apparent anomaly lies in the macrocyclic constrictive effect.⁸ It has been reported that saturated nitrogen donors in the smaller (13- and 14-membered) macrocycles exhibit abnormally large field strengths because the ring compresses the metal nitrogen bond.

Several low-spin six-coordinate iron(III) porphyrin

(36) A. Hudson and H. J. Whitfield, *Inorg. Chem.*, **6**, 1120 (1967).

(37) B. W. Dale, R. J. P. Williams, P. R. Edwards, and C. E. Johnson, *Trans. Faraday Soc.*, **64**, 3011 (1968).

complexes with imidazole or pyridine as the axial ligands have been studied.³⁸ Their isomer shift values at 77°K range from 0.27 to 0.35 mm/sec. The ΔE_q values are essentially temperature independent and range from 1.25 to 2.35 mm/sec with most values near 2.0 mm/sec. The *cs* values for some of the complexes measured at room temperature were lower than those reported at 77°K and gave values similar to those reported for the low-spin iron(III) complexes of this report. The ΔE_q values of the six-coordinate iron(III) complexes in Table I are similar to those found for the more complicated molecules.

A large number of iron(III) oxo bridged dimers containing various substituted porphyrins have been synthesized and their Mössbauer spectra recorded.³⁹ They all have closely similar *cs* values (0.40 ± 0.05 mm/sec) and ΔE_q values (0.60 ± 0.10 mm/sec), at 298°K. On the basis of the similarity of the structures, [Fe(TAAB)(OMe)₂]₂O should be the most suitable for comparison, but its ΔE_q value is significantly different. Although this complex contains an aromatic dianionic ligand (Figure 1, k), the presence of two sp³ carbon atoms in the ring gives rise to stereochemical complications which probably influence the ΔE_q value. The nonaromatic planar TAAB complex (Figure 1, j) gives values rather more similar to those of the porphyrins.

In general, the Mössbauer parameters for the complexes presented here are not significantly different from those involving porphyrin ligands. Using relatively simple model systems it has been possible to examine some of the factors influencing the Mössbauer spectrum of complexes with this important class of cyclic structures. The successful application of the concepts of partial center shift and partial quadrupole splitting to cyclic systems of varying symmetry and ring size will make the extension to more complicated systems particularly attractive. Even with tetradentate ligands of varied functionality each of the ligating groups exerts on the Mössbauer nuclide an effect which is relatively independent of the other groups present in the complex. Also as shown here, further correlation of *pcs* and *pqs* values with other parameters directly associated with the electronic structure of the complex may allow a better understanding of systems where such information is difficult to obtain.

Experimental Section

Physical Measurements. ⁵⁷Fe Mössbauer spectra were obtained with a conventional constant-acceleration spectrometer operated in the time mode, with a ⁵⁷Co(Cu) source. Experiments were performed with both source and absorber at room temperature. The spectrometer was calibrated with a sodium nitroprusside standard; Fe₂O₃ and iron metal were employed as secondary standards. Isomer shifts and quadrupole splittings were determined by inspection with an accuracy of ±0.01 mm/sec. A sample spectrum is shown in Figure 6. Isomer shifts are quoted relative to stainless steel (to convert to sodium nitroprusside, add 0.16 mm/sec). The absorber thickness was normally less than 75 mg/cm² of the compound. Air-sensitive samples were suitably encapsulated in an argon atmosphere to prevent reaction during the experiment.

The majority of the infrared spectra were obtained on a Perkin-Elmer Model 337 recording spectrometer using Nujol mulls between KBr disks. The cyanide stretching vibrations of the four low-spin cyano derivatives (Table I) were measured using Nujol

(38) L. M. Epstein, D. K. Straub, and C. Maricondi, *Inorg. Chem.*, **6**, 1720 (1967).

(39) M. A. Torrens, D. K. Straub, and L. M. Epstein, *J. Amer. Chem. Soc.*, **94**, 4160 (1972).

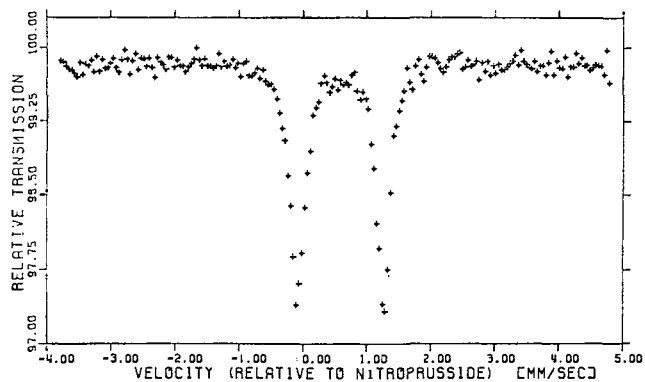


Figure 6. Mössbauer spectrum of $[\text{Fe}(1,3,7,10\text{-CT})(\text{CH}_3\text{CN})_2](\text{ClO}_4)_2$.

mulls between KBr disks on a Perkin-Elmer 457 spectrometer. The reference compound was $\text{Fe}([\text{14}]\text{1,3,8,10-tetraeneN}_4)(\text{CN})_2$ which gave a single absorption at $2099 \pm 4 \text{ cm}^{-1}$. This complex was mixed with the other complexes, and shifts were measured relative to it with an accuracy of $\pm 1 \text{ cm}^{-1}$.

The conductivities of the complexes were obtained by using an Industrial Instruments Model RC 16B conductivity bridge. The measurements were determined at 25° at 1000 Hz on $10^{-3} M$ solutions unless otherwise noted. The nitromethane solvent was purified according to standard procedures.⁴⁰

Solid-state magnetic moments were determined at room temperature under 33 mm of helium gas using the Faraday method.⁴¹ Proton magnetic resonance spectra (pmr) were obtained on Varian A60-A and HA-100 spectrometers.

Syntheses. All materials were reagent grade and used without further purification unless otherwise noted. The syntheses were carried out in a drybox and on the "bench top" under a blanket of nitrogen gas unless otherwise noted.

$[\text{Fe}([\text{14}]\text{4,11-dieneN}_4)(\text{Im})_2](\text{BPh})_2$. One gram of $[\text{Fe}([\text{14}]\text{4,11-dieneN}_4)(\text{CH}_3\text{CN})_2](\text{ClO}_4)_2$ was suspended in 10 ml of absolute ethanol, and excess imidazole was added. Gentle heating caused the solid to dissolve to produce a light green solution. The addition of excess of sodium tetraphenylborate and cooling caused the crystallization of the dark olive green complex. *Anal.* Calcd for $\text{C}_{70}\text{H}_{80}\text{N}_8\text{B}_2\text{Fe}$: C, 75.68; H, 7.26; N, 10.09; Fe, 5.03. Found: C, 75.30; H, 7.79; N, 9.26; Fe, 4.75. Ir (cm^{-1}) $\nu(\text{NH})$ 3300 s, 3120 w; $\nu(\text{C}=\text{N})$ 1610 m, 1590 m. $\Lambda(\text{CH}_3\text{NO}_2)$ $154 \text{ ohm}^{-1} M^{-1}$; diamagnetic.

$[\text{Fe}([\text{14}]\text{4,11-dieneN}_4)(\text{CN})_2](\text{CH}_3\text{CN})_2(\text{ClO}_4)_2$. One gram of $[\text{Fe}([\text{14}]\text{4,11-dieneN}_4)(\text{CH}_3\text{CN})_2](\text{ClO}_4)_2$ was dissolved in 50 ml of anhydrous methanol. To the resulting solution was added 0.3 g of NaCN, and the suspension was stirred rapidly for 30 min. The solvent was removed *in vacuo*, the dicyano complex was dissolved in CHCl_3 , and the excess NaCN and NaClO_4 were removed by filtration. Reduction of the volume and standing allowed the slow crystallization of the yellow dicyano complex as large plates. *Anal.* Calcd for $\text{C}_{18}\text{H}_{32}\text{N}_6\text{Fe}$: C, 55.23; H, 8.24; N, 21.47. Found: C, 54.36; H, 7.42; N, 21.26. Pmr in CDCl_3 (ppm), imine-CH, 2.04; gem-CH₃, 1.03, 1.17. Ir (cm^{-1}) $\nu(\text{N-H})$ 3200 s; $\nu(\text{C}=\text{N})$ 2071 s; $\nu(\text{N}=\text{C})$ 1635 w. $\Lambda(\text{CH}_3\text{NO}_2)$, $4 \text{ ohm}^{-1} M^{-1}$; diamagnetic.

$[\text{Fe}([\text{14}]\text{1,4,8,11-tetraeneN}_4)(\text{Im})_2](\text{BF}_4)_2$. One gram of $[\text{Fe}([\text{14}]\text{1,4,8,11-tetraeneN}_4)(\text{CH}_3\text{CN})_2](\text{PF}_6)_2$ ³ was partially dissolved in 50 ml of acetone, and excess imidazole was added. The solution

immediately turned brown. The trans imidazole complex crystallized upon the addition of excess LiBF_4 dissolved in acetone. Recrystallization from hot nitromethane yielded the pure brown crystalline solid. *Anal.* Calcd for $\text{C}_{22}\text{H}_{36}\text{N}_8\text{B}_2\text{F}_8\text{Fe}$: C, 41.16; H, 5.65; N, 17.45. Found: C, 40.81; H, 5.74; N, 17.68. Ir (cm^{-1}) $\nu(\text{N-H})$ 3340 s, 3140 m, $\nu(\text{N}=\text{C})$ 1640 w, 1620 s. $\Lambda(\text{CH}_3\text{NO}_2)$, $204 \text{ ohm}^{-1} M^{-1}$; diamagnetic.

$[\text{Fe}([\text{14}]\text{1,4,8,11-tetraeneN}_4)(\text{NO}_2)_2$. The nitro complex was made in the same manner as the imidazole derivative using excess NaNO_2 . The olive green acetone solution was reduced to dryness *in vacuo*, and the residue was taken up in chloroform. After filtration the chloroform solution was reduced to dryness and the crude green complex was recrystallized from hot absolute methanol. *Anal.* Calcd for $\text{C}_{16}\text{H}_{28}\text{N}_6\text{O}_4\text{Fe}$: C, 45.29; H, 6.65; N, 19.81. Found: C, 44.67; H, 6.73; N, 19.48. Ir (cm^{-1}) $\nu(\text{N}=\text{C})$ 1650 w, 1630 s; $\nu(\text{NO}_2^-)$ 1300 s, 1265 s. $\Lambda(\text{CH}_3\text{NO}_2)$, $6 \text{ ohm}^{-1} M^{-1}$; diamagnetic.

$[\text{Fe}(\text{Me}_2[\text{14}]\text{janeN}_4)(\text{CH}_3\text{CN})_2](\text{ClO}_4)_2$. This complex was prepared in a manner similar to that used for $[\text{Fe}([\text{14}]\text{janeN}_4)(\text{CH}_3\text{CN})_2](\text{BF}_4)_2$.⁴ To 300 ml of refluxing CH_3CN under N_2 was added 3.81 g (2.19×10^{-2} mol) of anhydrous iron(II) acetate. The suspension was stirred for 15 min, and 5.0 g (2.19×10^{-2} mol) of $\text{Me}_2[\text{14}]\text{janeN}_4$ was added. After 30 min both the iron salt and the ligand dissolved forming a pale green solution. Perchloric acid (70%), 6.3 g, was added dropwise producing a red-violet solution. Reducing the volume of the solution under vacuum with mild heat to about 100 ml, followed by addition of 200 ml of tetrahydrofuran and 100 ml of ether, yielded 5.0 g of the complex. *Anal.* Calcd for $\text{C}_{16}\text{H}_{34}\text{N}_6\text{Cl}_2\text{O}_8\text{Fe}$: C, 33.99; H, 6.06; N, 14.87. Found: C, 33.64; H, 6.10; N, 14.64. Ir (cm^{-1}) $\nu(\text{NH})$ 3250 s; $\nu(\text{C}=\text{N})$ 2250 w. $\Lambda(\text{CH}_3\text{CN})$, $308 \text{ ohm}^{-1} M^{-1}$; diamagnetic.

$[\text{Fe}(\text{Me}_2[\text{14}]\text{janeN}_4)(\text{CH}_3\text{CN})_2](\text{ClO}_4)_3$. Oxygen gas was bubbled through an acetonitrile solution containing $[\text{Fe}(\text{Me}_2[\text{14}]\text{janeN}_4)(\text{CH}_3\text{CN})_2](\text{ClO}_4)_2$ and a few milliliters of HClO_4 . The solution immediately turned yellow-brown, and the yellow $[\text{Fe}(\text{Me}_2[\text{14}]\text{janeN}_4)(\text{CH}_3\text{CN})_2](\text{ClO}_4)_3$ complex crystallized. *Anal.* Calcd for $\text{C}_{16}\text{H}_{34}\text{N}_6\text{Cl}_3\text{O}_{12}\text{Fe}$: C, 28.91; H, 5.16; N, 12.64. Found: C, 28.82; H, 5.07; N, 12.56. Ir (cm^{-1}) $\nu(\text{NH})$ 3230 s; $\nu(\text{C}=\text{N})$ 2230 m, 2300 m. $\Lambda(\text{CH}_3\text{CN})$, $384 \text{ ohm}^{-1} M^{-1}$, $\mu_{\text{eff}} = 2.42 \text{ BM}$.

$[\text{Fe}(\text{TAAB})(\text{CH}_3\text{CN})_2](\text{ClO}_4)_2$. *o*-Aminobenzaldehyde (16.0 g, 0.19 mol) was dissolved in 40 ml of absolute ethanol, and the solution was heated to reflux. A solution containing 8.3 g (0.068 mol) of anhydrous FeCl_2 and 0.3 ml of concentrated aqueous HCl in ethanol was slowly added to the aldehyde solution. After refluxing for 6 hr a small amount of $[\text{Fe}(\text{TAAB})(\text{CH}_3\text{CN})_2]\text{FeCl}_4$ precipitated from the dark green solution. Cooling to -10° resulted in the crystallization of additional complex which was removed by filtration, washed with ethanol, and dried under N_2 . The yield of the black $[\text{Fe}(\text{TAAB})(\text{CH}_3\text{CN})_2]\text{FeCl}_4$ was 3.7 g. This material was dissolved in a minimum amount of CH_3CN ; excess LiClO_4 and a small amount of ether were added. Dark red $[\text{Fe}(\text{TAAB})(\text{CH}_3\text{CN})_2](\text{ClO}_4)_2$ slowly crystallized. *Anal.* Calcd for $\text{C}_{32}\text{H}_{26}\text{N}_6\text{Cl}_2\text{O}_8\text{Fe}$: C, 51.30; H, 3.47; N, 11.20. Found: C, 49.47; H, 3.40; N, 10.98. Ir (cm^{-1}) C=N and phenyl, 1600 s, 1580 s, 1560 s.

Preparation of the remaining complexes with macrocycles $[\text{14}]\text{janeN}_4$,⁴ $[\text{14}]\text{4,11-dieneN}_4$,² $[\text{14}]\text{1,4,11-triene}$,³ $[\text{14}]\text{1,4,8,11-tetraeneN}_4$,³ $[\text{14}]\text{1,3,7,11-tetraeneN}_4$,⁵ $[\text{14}]\text{1,3,8-trieneN}_4$,⁵ $[\text{14}]\text{1,3,8,10-tetraeneN}_4$,⁶ $[\text{14}]\text{1,3,7,10-tetraeneN}_4$,⁵ and $[\text{14}]\text{janeS}_4$ ⁷ were previously described. The μ -oxo bridged dimeric complexes with the TAAB ligand were prepared as described earlier.⁶

Acknowledgment. These studies were supported by U. S. Public Health Services Grant No. GM 10040 from the National Institute of General Medical Sciences. Part of the information contained in this article was developed during the course of work under Contract AT(07-2)-1 with the U. S. Atomic Energy Commission.

(40) G. A. Olah, S. J. Kuhn, S. H. Flood, and B. A. Hardie, *J. Amer. Chem. Soc.*, **86**, 1039 (1964).

(41) L. F. Lindoy, V. Katovic, and D. H. Busch, *J. Chem. Educ.*, **49**, 117 (1972).